

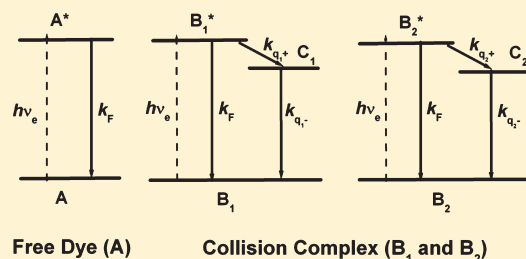
Structural Heterogeneity in the Collision Complex between Organic Dyes and Tryptophan in Aqueous Solution

Qinfang Sun, Rong Lu, and Anchi Yu*

Department of Chemistry, Renmin University of China, Beijing 100872, People's Republic of China

Supporting Information

ABSTRACT: The heterogeneity on photoinduced electron transfer (PET) kinetics between a labeled fluorophore and an amino acid residue has been extensively studied in biopolymers. However in aqueous solutions, the heterogeneity on PET kinetics between a fluorophore and a quencher has rarely been reported. Herein, we selected four commonly used fluorophores, such as tetramethylrhodamine (TMR), Rhodamine B (RhB), Alexa fluor 546 (Alexa546), and Atto655, and studied their respective PET kinetics in 50 mM tryptophan solutions with femtosecond transient absorption spectroscopy to explore the structural heterogeneity in their corresponding collision complexes. We measured the decay of the first excited electronic state of respective fluorophore with and without 50 mM tryptophan in aqueous solutions, and derived the charge separation rate in their corresponding collision complexes. We found that the PET process of all selected fluorophores in 50 mM tryptophan solutions has two charge separation rates, which indicates that the relevant states in the collision complex between respective fluorophore and tryptophan have strong structural heterogeneity. These femtosecond PET measurements are in agreement with Vaiana's molecular dynamics simulation (*J. Am. Chem. Soc.* **2003**, *125*, 14564). In addition, with the obtained PET kinetic parameters, we derived the relative brightness of the collision complex between respective fluorophore and tryptophan, which are important parameters for the PET based fluorescence correlation spectroscopy study involving these fluorophores in biopolymers.



INTRODUCTION

Photoinduced electron transfer based fluorescence correlation spectroscopy (PET-FCS) is a powerful tool for studying the conformational dynamics of biopolymers.^{1–24} Because it requires contact formation between the fluorophore and the quencher at a van der Waals distance of subnanometer scale,²³ PET has been an elegant alternation to the conventional fluorescence resonance energy transfer (FRET). In the traditional two-state PET-FCS model, researchers generally assumed the brightness of the dark species to be zero so that they could extract both the forward and reverse rate constants from a single PET-FCS curve.⁹ However, our recent studies suggested that the PET-FCS data alone are no longer sufficient to extract the forward and reverse rate constants when more accurate physical interpretation is considered.^{24–26} The brightness of the dark species has to be determined with an additional experiment, i.e., transient absorption, transient fluorescence, and/or ensemble static fluorescence measurement, so as to obtain the correct forward and reverse rate constants.^{24,25}

Many fluorophores such as Alexa fluor,^{18,27} 2-aminopurine,^{5,6,28–30} Bodipy-FL,^{11,31} coumarin,³² fluorescein,^{3,17,33–36} oxazine,^{2,4,9,10,14,19,21,26,37–40} rhodamine,^{7,20,24,25,40,41} and pyrene^{42–45} have been reported to have PET interaction with the nucleobase guanosine or the amino acid tryptophan. Depending on the reduction potential of the fluorophore used, the efficient PET can occur between the first excited singlet electronic state of the fluorophore and the ground electronic state of the quencher.^{12,30,32} Two mechanisms,

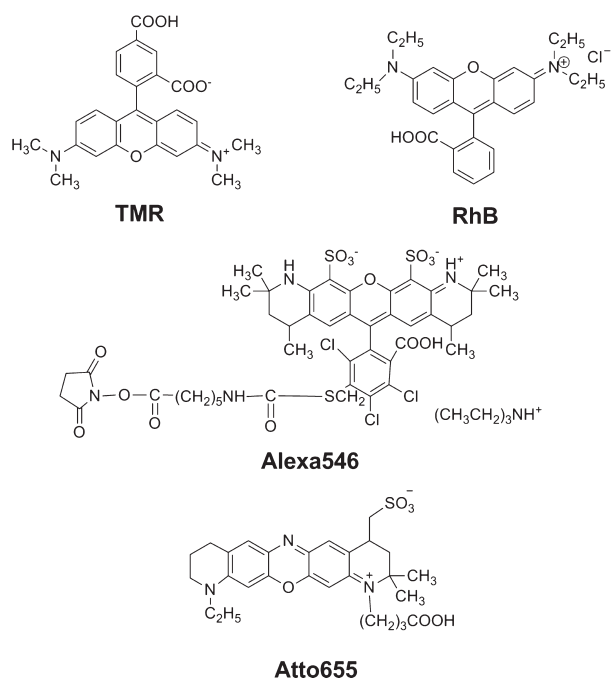
so-called static and dynamic quenching, have been proposed for the deactivation of the excited fluorophore.^{5,23,32,40} However, Zewail et al. pointed out that this distinction depends on the actual time scale of the experimental methods.²⁹ Moreover, Sauer and co-workers performed molecular dynamics simulation study on the fluorescence quenching of Rhodamine 6G (R6G) and MR121 in the presence of tryptophan in aqueous solutions.⁴⁶ They found that the relevant states in the collision complex between R6G or MR121 and tryptophan have several different geometries.⁴⁶ Therefore, the PET process between R6G or MR121 and tryptophan should exhibit strong heterogeneity in their kinetics.

The heterogeneity on PET kinetics between a labeled fluorophore and an amino acid residue has been extensively studied in biopolymers.^{47–55} However, in the literature, we have not found any femtosecond study involving the heterogeneity on the PET process between a fluorophore and a quencher in aqueous solutions. In this work, we selected four commonly used fluorophores, such as tetramethylrhodamine (TMR), Rhodamine B (RhB), Alexa fluor 546 (Alexa546), and Atto655 (Scheme 1), and studied their respective ultrafast PET kinetics in the presence of 50 mM tryptophan solution with femtosecond transient absorption and/or fluorescence spectroscopy to explore the structural heterogeneity in their corresponding collision

Received: October 19, 2011

Revised: December 8, 2011

Published: December 12, 2011

Scheme 1. Molecular Structure of TMR, RhB, Alexa546, and Atto655^a

^a The chemical structure of Atto655 was reprinted with permission from ref 60. Copyright 2011 Royal Society of Chemistry.

complexes. We measured the decay of the first excited electronic state of respective fluorophore in the absence and in the presence of 50 mM tryptophan so that we were able to derive the charge separation rate in their corresponding collision complexes. We found that the PET process of all selected fluorophores in the presence of 50 mM tryptophan has two charge separation rates, which indicates that the relevant states in the collision complex between respective fluorophore and tryptophan have strong structural heterogeneity. The charge separation rates for the two relevant states in the collision complex between TMR or Alexa546 and tryptophan are about 1.4×10^{11} and $7.6 \times 10^9 \text{ s}^{-1}$, the charge separation rates for the two relevant states in the collision complex between RhB and tryptophan are about 0.6×10^{11} and $8.3 \times 10^9 \text{ s}^{-1}$, and the charge separation rates for the two relevant states in the collision complex between Atto655 and tryptophan are about 2.0×10^{12} and $3.2 \times 10^{11} \text{ s}^{-1}$. With these obtained PET kinetic parameters, we derived the relative brightness of the collision complex between respective fluorophore and tryptophan, which are important parameters for the PET-FCS study involving these fluorophores in biopolymers.

EXPERIMENTAL SECTION

Materials. Tetramethylrhodamine (TMR), Rhodamine B (RhB), and tryptophan were purchased from Sigma-Aldrich, St. Louis, MO, and used as received. Alexa fluor 546 (Alexa546) was purchased from Invitrogen, Carlsbad, CA, and used as received. Atto655 was purchased from Atto-Tec GmbH, Siegen, Germany, and used as received. One× TE buffer (pH 8.0) was diluted from 100× TE (Sigma-Aldrich, St. Louis, MO). Ultrapure water ($18.2 \text{ M}\Omega \cdot \text{cm}^{-2}$) was obtained through a Milli-Q water purification system (Millipore, Billerica, MA).

Static Absorption and Fluorescence Measurements. Static absorption spectra were recorded by a Cary 50 UV–vis spectrometer (Varian, Forest Hill, Victoria, Australia). Static fluorescence spectra were recorded on a LS-55 luminescence spectrometer (Perkin-Elmer, Waltham, MA). To record the weak fluorescence, a charge-coupled device (CCD; Spec10:400B, Princeton Instruments, Acton, MA) and laser excitation were employed.

Femtosecond Transient Absorption Measurements. We used an amplified Ti:sapphire laser system (Spitfire, Spectra Physics, Mountain View, CA), which generates about 100 fs laser pulses at 840 nm with a repetition rate of 1 kHz and an average power of around 1.0 W. These fundamental pulses were used to pump an optical parametric amplifier (OPA) as well as to generate the white light continuum. The OPA pulses were about 100 fs and could be tuned from 450 to 700 nm. The white light continuum was generated in a spinning fused-silica disk with the 840 nm pump pulse, and its spectrum covers the range from 420 to 750 nm. The OPA outputs were used as the pump pulses, and the white light continuum were used as the probe pulses. The timing between the pump and probe pulses was controlled using a motorized translation stage (M-ILS250CC, Newport, Irvine, CA). The pump and probe beams were noncollinearly focused into the sample cell using two achromatic lenses (300 mm focal length for pump and 100 mm focal length for probe, respectively). At the sample position, the average powers were about 0.5 mW for pump beam and around $10 \mu\text{W}$ for the white light continuum probe beam. The signals were collected by a large area adjustable gain balanced photoreceiver (2307, Newport, Irvine, CA), which was attached to the output port of a monochromator (SP2358, Princeton Instruments, Acton, MA) and sent to a lock-in amplifier (SR850, Stanford Research Systems, Sunnyvale, CA) where it was synchronized by an optical chopper (75160, Newport, Irvine, CA). The chopped frequency was 160 Hz. The polarization of the pump pulses was set at 54.7° with respect to the polarization of the probe pulses to get rid of the molecular reorientation effect. The time resolution for this femtosecond transient absorption apparatus was estimated to be about 150 fs through the cross-correlation between the pump and probe pulses in buffer solution.

Femtosecond Fluorescence Up-Conversion Measurements. Our femtosecond fluorescence up-conversion setup was a typical apparatus as widely reported in the literature.^{29,56,57} Briefly, the fluorescence of the sample was initiated by the pump pulses from the OPA output (530 nm, 100 fs) and collected by a pair of 90° -off parabolic mirrors (Edmund Optics Inc., Barrington, NJ) and then mixed with the gate pulse (840 nm, 100 fs) in a 0.5 mm thick BBO crystal. Polarization of the pump pulses was rotated with respect to the gate pulses by 54.7° (magic angle) using a $\lambda/2$ waveplate (10RP52-1, Newport, Irvine, CA). The fluorescence and the gate were noncollinearly focused to the BBO crystal with an angle of about 15° . The up-conversion signal was sent to a monochromator (SP2358, Princeton Instruments, Acton, MA) and detected by a photomultiplier tube (R955, Hamamatsu, Hamamatsu City, Japan). Finally, the signal from the photomultiplier tube was averaged by a boxcar integrator (4121B, EG&G, Gaithersburg, MD). The average power for the pump pulses at the sample position was about 0.5 mW, and the average power for the gate pulses at the BBO position was about 100 mW. The timing between the pump pulses and the gate pulses was controlled with a motorized translation stage (M-ILS250CC, Newport, Irvine, CA). The time resolution for this femtosecond fluorescence up-conversion apparatus was estimated to

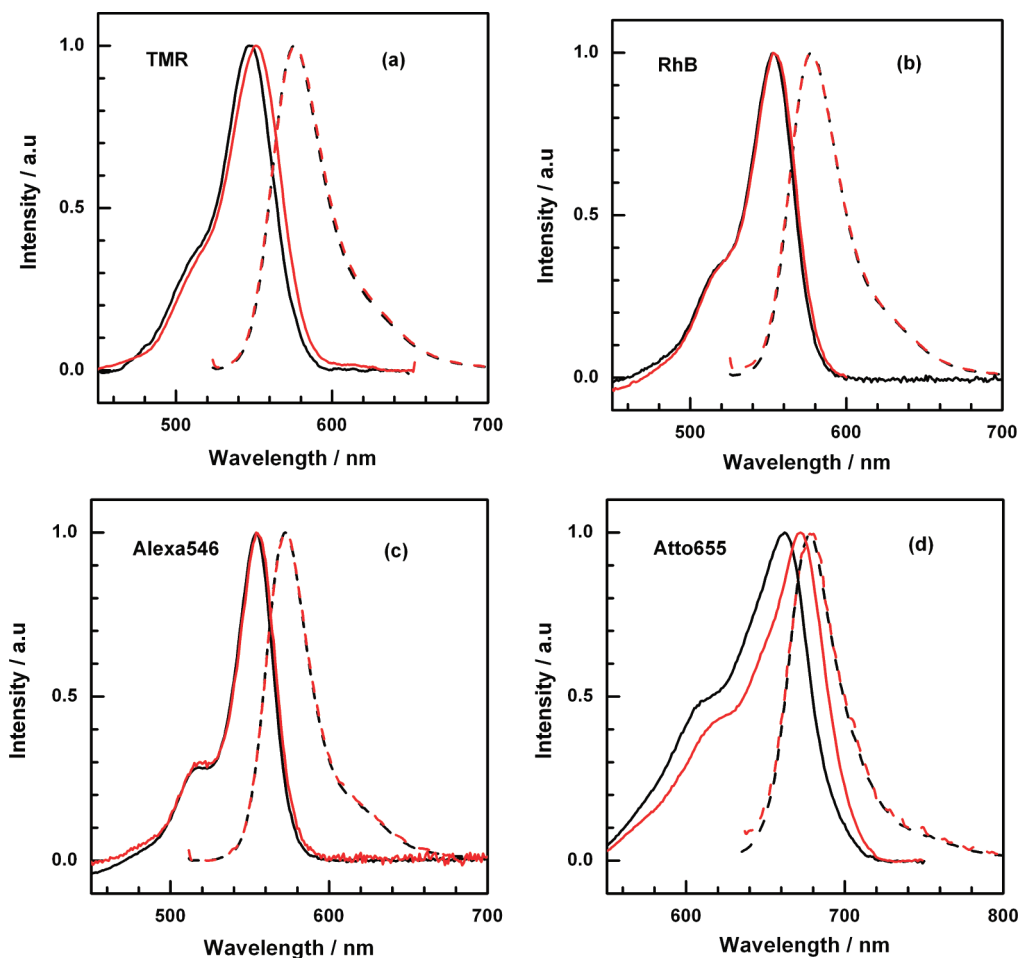


Figure 1. Normalized static absorption (solid line) and fluorescence (dash line) spectra of TMR (a), RhB (b), Alexa546 (c), and Atto655 (d) in the absence (black line) and in the presence (red line) of 50.0 mM tryptophan in $1 \times$ TE buffer.

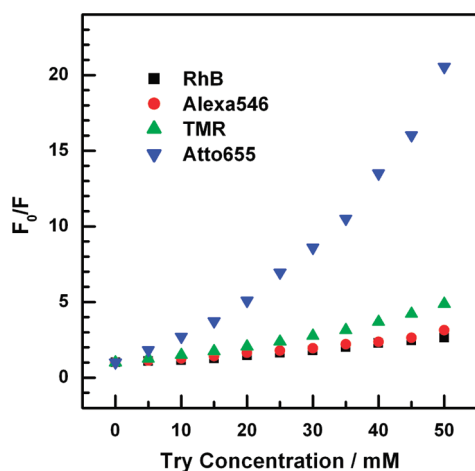


Figure 2. Static bimolecular Stern–Volmer plot of RhB (■), Alexa546 (●), TMR (▲), and Atto655 (▼) in the presence of tryptophan in $1 \times$ TE buffer.

be around 500 fs from the cross-correlation between the scattered pump and gate pulses.

In static absorption and fluorescence spectroscopy measurements, the concentrations of the samples were adjusted to have

an optical density of about 0.1 at their maximum absorption positions in a 1 cm path length sample cell. In femtosecond transient absorption spectroscopy measurements, the concentrations of the samples were adjusted to have an optical density of about 0.1 at their maximum absorption positions in a 1 mm path length sample cell. In femtosecond fluorescence up-conversion measurements, the concentrations of the samples were adjusted to have an optical density of about 0.5 at their maximum absorption positions in a 1 mm path length sample cell. To keep the sample solution fresh, a homemade magnet stirring bar was placed inside the sample cell and rotated by an external magnet motor. The static absorption spectra of the sample were measured before and after each ultrafast kinetic measurement to check the sample's quality and stability. The data were disregarded when the sample degradation was greater than 5%.

RESULTS AND DISCUSSION

Ensemble Static Absorption and Fluorescence Measurements.

The evidence for the formation of a ground state complex between a fluorophore and a quencher can be revealed through its ensemble static absorption and fluorescence spectra.^{2,39,40,58} Figure 1 displays the ensemble static absorption and fluorescence spectra of TMR, RhB, Alexa546, and Atto655 with and without 50 mM tryptophan in aqueous solutions, respectively. From the spectroscopic data shown

in Figure 1, it can be found that the interaction between respective fluorophore and tryptophan are quite different. The absorption maximum of Atto655 or TMR in 50 mM tryptophan solution has an obvious red-shift, while that of Alexa546 or RhB has only a slight red-shift. To further study the interaction between respective fluorophore and tryptophan, we recorded the fluorescence intensity Stern–Volmer plots of all selected fluorophores in the presence of tryptophan in aqueous solutions, as shown in Figure 2. Clearly, Atto655 shows the most pronounced quenching efficiency by tryptophan, and all Stern–Volmer plots shown in Figure 2 have upward curvatures. The reason for the nonlinearity of a Stern–Volmer plot has been discussed thoroughly.^{40,46} In the literature, it has been suggested that the deviation from linearity with increasing quencher concentration in a Stern–Volmer plot is due to different populations of fluorophores.⁴⁶ Both the pronounced quenching efficiency of Atto655 by tryptophan and the dramatic red-shift of the absorption maximum of Atto655 in 50 mM tryptophan solution indicate that the PET process between Atto655 and tryptophan is different from that of TMR, RhB, and Alexa546.

Ultrafast Excited-State Decay Measurements. To understand the PET process between respective fluorophore and tryptophan, we measured the kinetic trace of each fluorophore in the absence and in the presence of 50 mM tryptophan in aqueous solutions by monitoring their respective transient absorption of the $S_1 \rightarrow S_n$ transition after the fluorophore was

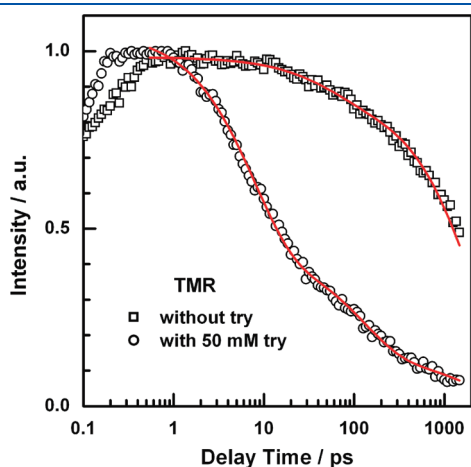


Figure 3. Magic-angle femtosecond pump–probe transients of TMR in the absence (\square) and in the presence (\circ) of 50.0 mM tryptophan in $1 \times$ TE buffer. Pump, 530 nm; probe, 420 nm.

excited into its first excited electronic state.⁵⁹ Figure 3 shows the decay of the first excited electronic state of TMR alone and in the presence of 50 mM tryptophan. The transient absorption of TMR without 50 mM tryptophan can be fitted by two exponential decays with the parameters listed in Table 1. The 2250 ps lifetime is consistent with the lifetime of TMR alone in aqueous solution measured by time correlated single photon counting technique (TCSPC, Figure S1 in the Supporting Information) and in the literature.⁵⁸ The fast 50 ps component is most likely due to the interaction between TMR molecules because its amplitude reduced with the decrease of the TMR concentration.²⁵ However, we were unable to totally get rid of it since the transient absorption measurement required rather high sample concentration. The transients of TMR in the presence of 50 mM tryptophan needs three exponential decays to be fitted and the fitting parameters are also listed in Table 1. The lifetime of the two fast components (7 and 125 ps) in the presence of 50 mM tryptophan is not the same as that of TMR alone (50 ps). More importantly, within the experimental error, the lifetime and the amplitude of these two fast decay components in 50 mM tryptophan did not vary with the variation of the TMR concentration. To confirm that the measured decays in the transient absorption were associated with the initially populated first excited electronic state of TMR and the absorption of its charge separation state has no significant effect on the measured decays,⁵⁹ we further performed the femtosecond fluorescence up-conversion measurement on TMR in 50 mM tryptophan solution, as shown in Figure 4. The femtosecond fluorescence up-conversion measurement gave an identical result as the femtosecond transient absorption measurement (Table 1). Thus, the 7 and 125 ps decay components are the excited electronic state lifetime of the collision complex between TMR and tryptophan, while the 2250 ps decay component is the excited electronic state lifetime of free TMR.

Similarly, we measured the decays of the first excited electronic state of RhB, Alexa546, and Atto655 in the absence and in the presence of 50 mM tryptophan in aqueous solutions, as shown in Figures 5 and 6. The PET kinetics of RhB and Alexa546 in the presence of 50 mM tryptophan are very similar to that of TMR in 50 mM tryptophan, which both have ~ 10 ps and ~ 100 ps decay components in their collision complexes (Table 1). More interestingly, the amplitude ratios of the two fast decay components in the PET kinetics between TMR, RhB, or Alexa546 and tryptophan are about the same (both are about 2.3:1, Table 1). While the PET kinetics between Atto655 and tryptophan is much faster than that of TMR in tryptophan (Table 1). The different time

Table 1. Excited Electronic State Decay Parameters for TMR, RhB, Alexa546, and Atto655 in the Absence and in the Presence of 50.0 mM Tryptophan (try) in $1 \times$ TE Buffer

	[try] (mM)	a_1	τ_1 (ps)	a_2	τ_2 (ps)	a_3	τ_3 (ps) ^a	$\langle \tau \rangle$ (ps) ^b
TMR ^c	0.0			0.10	50	0.90	2250	
	50.0	0.60 (0.59)	7.0 (4.5)	0.27 (0.27)	125 (115)	0.13 (0.14)	2250 (2250)	44 (39)
RhB	0.0	0.08	1.3	0.05	70	0.87	1300	
	50.0	0.41	18.0	0.17	110	0.42	1300	45
Alexa546	0.0	0.08	3.3	0.06	75	0.86	3150	
	50.0	0.43	7.2	0.19	125	0.38	3150	43
Atto655	0.0			0.09	40	0.91	1800	
	50.0	0.32	0.5	0.61	3.1	0.07	1800	2.2

^a Fixed to match the lifetime obtained by time correlated single photon counting measurements. ^b $\langle \tau \rangle = (a_1\tau_1 + a_2\tau_2)/(a_1 + a_2)$, the averaged excited electronic state lifetime of the collision complex. ^c Data listed in parentheses were obtained from femtosecond fluorescence up-conversion measurements

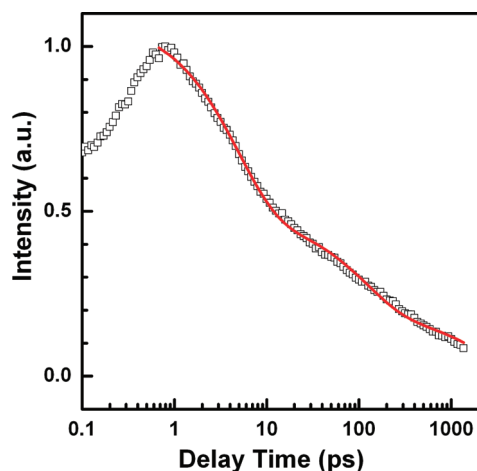


Figure 4. Magic-angle femtosecond fluorescence up-conversion signals of TMR in the presence of 50.0 mM tryptophan in $1 \times$ TE buffer. Pump, 530 nm; probe, 585 nm.

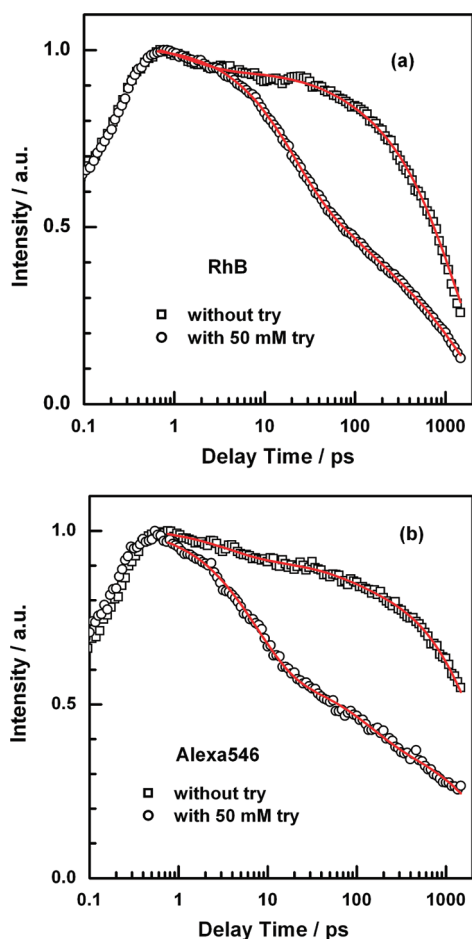


Figure 5. Magic-angle femtosecond pump-probe transients of RhB (a) and Alexa546 (b) in the absence (\square) and in the presence (\circ) of 50.0 mM tryptophan in $1 \times$ TE buffer. Pump, 530 nm; probe, 420 nm.

scales in PET kinetics between TMR and Atto655 in tryptophan solutions were probably due to their different reduction potential in aqueous solution. In the literature, we can not find the reduction potential of TMR and Atto655. However, we found

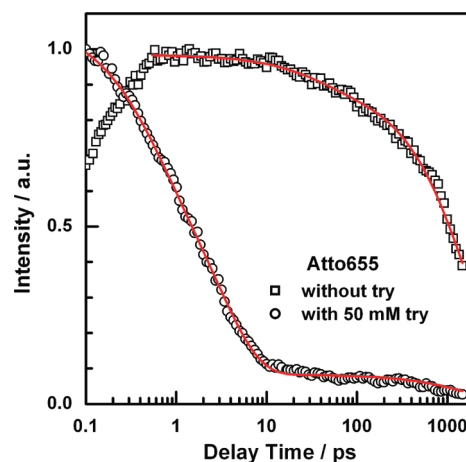


Figure 6. Magic-angle femtosecond pump-probe transients of Atto655 in the absence (\square) and in the presence (\circ) of 50.0 mM tryptophan in $1 \times$ TE buffer. Pump, 630 nm; probe, 530 nm.

that the reduction potentials of MR121 (similar to Atto655) and R6G (close to TMR) were reported to be -0.42 V (vs SCE) and -0.95 V (vs SCE).²³ Moreover, we have used the reduction potential of -0.42 V (vs SCE) for Atto655 to calculate the charge separation and recombination rates of the collision complex between Atto655 and tryptophan and the collision complex between Atto655 and guanosine, which is quite consistent with our femtosecond transient absorption measurements.²⁶

Structural Heterogeneity in the Collision Complex. In this work, we measured the ultrafast PET kinetics of TMR, RhB, Alexa546, and Atto655 in tryptophan solutions with femtosecond transient absorption spectroscopy. We found that all PET kinetics in their collision complexes exhibit nonexponential decay characteristics (Table 1). The nonexponential decay characteristic on the PET kinetics between respective fluorophore and tryptophan probably indicates that there exist several relevant states in their corresponding collision complex. In 2003, Sauer and co-workers performed a MD simulation study on the fluorescence quenching of R6G and MR121 in tryptophan solutions.⁴⁶ They found that the relevant states in the collision complex between R6G or MR121 and tryptophan have several different geometries. From the molecular structure shown in Scheme 1, it can be found that TMR, RhB, and Alexa546 are all rhodamine derivative dyes, while Atto655 is an oxazine derivative dye,⁶⁰ and its molecular structure is very similar to that of MR121. Therefore, our ultrafast PET measurements are in good agreement with Vaiana's MD simulation.⁴⁶ Besides, from the data listed in Table 1 and the kinetic traces shown in Figure 3, Figures 5 and 6, it can also be found that the nonexponential decay characteristic on the PET kinetics between Atto655 and tryptophan is obviously different from that of TMR, RhB, and Alexa546 in 50 mM tryptophan solutions. This also agrees with Vaiana's MD simulation on the fluorescence quenching of R6G and MR121 in tryptophan solutions.⁴⁶ They found that the normalized probability distribution of the R6G/tryptophan complex extends to a longer distance than that of the MR121/tryptophan complex due to the interaction geometries between tryptophan and the phenyl ring and ester group in R6G.⁴⁶ Thus, we concluded that the different relevant states in the collision complex between TMR, RhB, Alexa546, or Atto655 and tryptophan are probably the main source for the nonexponential decay

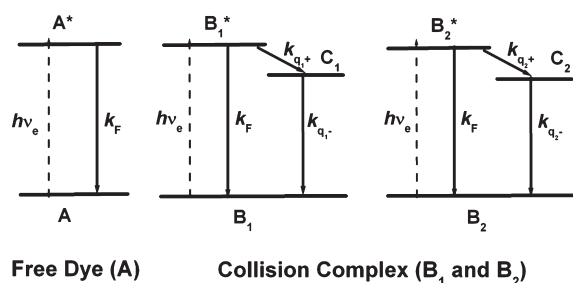


Figure 7. Dynamic model for radiative and nonradiative (PET) pathways of excited fluorophores in the presence of 50 mM tryptophan in $1 \times$ TE buffer.

characteristic in their PET kinetics. That is, the structure of the collision complex between respective fluorophore and tryptophan has strong heterogeneity.

With the PET scheme displayed in Figure 7 and the data listed in Table 1, we derived the charge separation rates of the relevant states (B_1 and B_2) in the collision complex between TMR, RhB, Alexa546, or Atto655 and tryptophan. The charge separation rates for the two relevant states in the collision complex between TMR or Alexa546 and tryptophan are around 1.4×10^{11} and $7.6 \times 10^9 \text{ s}^{-1}$, the charge separation rates for the two relevant states in the collision complex between RhB and tryptophan are around 0.6×10^{11} and $8.3 \times 10^9 \text{ s}^{-1}$, and the charge separation rates for the two relevant states in the collision complex between Atto655 and tryptophan are around 2.0×10^{12} and $3.2 \times 10^{11} \text{ s}^{-1}$.

Relative Brightness of the Collision Complex. Consider a chemical relaxation



where A is a fluorescent bright species, B is a dark species, and k_+ and k_- are the forward and reverse relaxation rate constants. The equilibrium constant is

$$K = \frac{k_+}{k_-} = \frac{C_B}{C_A} \quad (2)$$

where C_A and C_B are the concentration of species A and B, respectively. In a PET-FCS experiment, the autocorrelation function could be fitted by^{25,26}

$$G(t) = G_D(t) \times \left(1 + \alpha \exp\left(-\frac{t}{\tau}\right) \right) \quad (3)$$

where $G_D(t)$ is the term that describes the molecular diffusion,

$$\tau = \frac{1}{k_+ + k_-} \quad (4)$$

and

$$\alpha = \frac{(1 - Q)^2 K}{(1 + KQ)^2} \quad (5)$$

where Q is the relative brightness of B with respect to A. According to the PET scheme shown in Figure 7, the value of Q is²⁵

$$Q = \frac{k_F}{k_F + k_{q+}} = \frac{\tau}{\tau_0} \quad (6)$$

where k_F is the fluorescence rate of fluorophore without tryptophan, k_{q+} is the charge separation rate of the collision complex

between fluorophore and tryptophan, τ_0 is the fluorescence lifetime of fluorophore without tryptophan, and τ is the fluorescence lifetime of fluorophore with tryptophan. In a recent study, we analyzed the relationship between α and $k_+/(k_+ + k_-) = K/(1 + K)$, and we found that the $Q = 0$ assumption introduces serious error on the relationship between α and K when species B has a finite brightness.²⁶ Especially, when $k_+/(k_+ + k_-) \rightarrow 1$, α goes to a wrong limit of infinity instead of its correct value of zero. With a finite Q , one α value should generally correspond to two equilibrium constants as it should be, but the $Q = 0$ assumption would predict a one to one correspondence between α and K . Therefore, we ought to be cautious on whether the finite brightness of the dark species can be neglected or not even though Q was tiny. With the data listed in Table 1 and eq 6, we derived the averaged values $Q = 0.020$ for the collision complex between TMR and tryptophan, $Q = 0.035$ for the collision complex between RhB and tryptophan, $Q = 0.014$ for the collision complex between Alexa546 and tryptophan, and $Q = 0.001$ for the collision complex between Atto655 and tryptophan. These Q values are important parameters for the PET-FCS study involving these fluorophores in biopolymers.

CONCLUSIONS

In summary, we have selected four commonly used fluorophores, such as TMR, RhB, Alexa546, and Atto655, and studied their PET kinetics in 50 mM tryptophan solutions with femtosecond transient absorption spectroscopy. We measured the decay of the first excited electronic state of the respective fluorophore in the absence and in the presence of 50 mM tryptophan in aqueous solutions. We found that the PET process of all selected fluorophores in the presence of 50 mM tryptophan has two charge separation rates, suggesting that the relevant states in the collision complex between respective fluorophore and tryptophan have strong structural heterogeneity. The charge separation rates for the two relevant states in the collision complex between TMR or Alexa546 and tryptophan are about 1.4×10^{11} and $7.6 \times 10^9 \text{ s}^{-1}$, the charge separation rates for the two relevant states in the collision complex between RhB and tryptophan are about 0.6×10^{11} and $8.3 \times 10^9 \text{ s}^{-1}$, and the charge separation rates for the two relevant states in the collision complex between Atto655 and tryptophan are about 2.0×10^{12} and $3.2 \times 10^{11} \text{ s}^{-1}$. These femtosecond PET measurements are in good agreement with Vaiana's MD simulation on the fluorescence quenching of R6G and MR121 by tryptophan in aqueous solutions.⁴⁶ In addition, with the obtained PET kinetic parameters, we derived the averaged relative brightness values $Q = 0.020$ for the collision complex between TMR and tryptophan, $Q = 0.035$ for the collision complex between RhB and tryptophan, $Q = 0.014$ for the collision complex between Alexa546 and tryptophan, and $Q = 0.001$ for the collision complex between Atto655 and tryptophan. These Q values are important parameters for the PET-FCS study involving these fluorophores in biopolymers.

ASSOCIATED CONTENT

S Supporting Information. Fluorescence decay time profiles of dyes in $1 \times$ TE buffer obtained by time correlated single photon counting measurements and the excited state decay time profiles of Atto655 in the presence of different concentrations of tryptophan in $1 \times$ TE buffer. This material is available free of charge via the Internet at <http://pubs.acs.org>.

AUTHOR INFORMATION

Corresponding Author

*Phone: +86-10-6251-4601. Fax: +86-10-6251-6444. E-mail: a.yu@chem.ruc.edu.cn.

ACKNOWLEDGMENT

This work was supported by the National Natural Science Foundation of China (20733001, 20803092) and by the Fundamental Research Funds for the Central Universities and the Research Funds of Renmin University of China (10XNI007, 10XNJ047).

REFERENCES

- Neuweiler, H.; Sauer, M. *Curr. Pharm. Biotechnol.* **2004**, *5*, 285–298.
- Heinlein, T.; Knemeyer, J. P.; Piester, O.; Sauer, M. *J. Phys. Chem. B* **2003**, *107*, 7957–7964.
- Nazarenko, I.; Pires, R.; Lowe, B.; Obaidy, M.; Rashtchian, A. *Nucleic Acids Res.* **2002**, *30*, 2089–2095.
- Neuweiler, H.; Schulz, A.; Bohmer, M.; Enderlein, J.; Sauer, M. *J. Am. Chem. Soc.* **2003**, *125*, 5324–5330.
- Rachofsky, E. L.; Osman, R.; Ross, J. B. A. *Biochemistry* **2001**, *40*, 946–956.
- Rachofsky, E. L.; Seibert, E.; Stivers, J. T.; Osman, R.; Ross, J. B. A. *Biochemistry* **2001**, *40*, 957–967.
- Edman, L.; Mets, U.; Rigler, R. *Proc. Natl. Acad. Sci. U.S.A.* **1996**, *93*, 6710–6715.
- Kelley, S. O.; Barton, J. K. *Science* **1999**, *283*, 375–381.
- Kim, J.; Doose, S.; Neuweiler, H.; Sauer, M. *Nucleic Acids Res.* **2006**, *34*, 2516–2527.
- Knemeyer, J. P.; Marme, N.; Sauer, M. *Anal. Chem.* **2000**, *72*, 3717–3724.
- Kurata, S.; Kanagawa, T.; Yamada, K.; Torimura, M.; Yokomaku, T.; Kamagata, Y.; Kurane, R. *Nucleic Acids Res.* **2001**, *29*, e34.
- Lewis, F. D.; Letsinger, R. L.; Wasielewski, M. R. *Acc. Chem. Res.* **2001**, *34*, 159–170.
- Lewis, F. D.; Wu, T. F.; Zhang, Y. F.; Letsinger, R. L.; Greenfield, S. R.; Wasielewski, M. R. *Science* **1997**, *277*, 673–676.
- Rogers, J. M. G.; Poishchuk, A. L.; Guo, L.; Wang, J.; DeGrado, W. F.; Gai, F. *Langmuir* **2011**, *27*, 3815–3821.
- Schuettpelz, M.; Schoening, J. C.; Doose, S.; Neuweiler, H.; Peters, E.; Staiger, D.; Sauer, M. *J. Am. Chem. Soc.* **2008**, *130*, 9507–9513.
- Hudgins, R. R.; Huang, F.; Gramlich, G.; Nau, W. M. *J. Am. Chem. Soc.* **2002**, *124*, 556–564.
- Kaji, T.; Ito, S.; Iwai, S.; Miyasaka, H. *J. Phys. Chem. B* **2009**, *113*, 13917–13925.
- Chen, H.; Rhoades, E.; Butler, J. S.; Loh, S. N.; Webb, W. W. *Proc. Natl. Acad. Sci. U.S.A.* **2007**, *104*, 10459–10464.
- Doose, S.; Neuweiler, H.; Barsch, H.; Sauer, M. *Proc. Natl. Acad. Sci. U.S.A.* **2007**, *104*, 17400–17405.
- Eggeling, C.; Fries, J. R.; Brand, L.; Gunther, R.; Seidel, C. A. M. *Proc. Natl. Acad. Sci. U.S.A.* **1998**, *95*, 1556–1561.
- Neuweiler, H.; Doose, S.; Sauer, M. *Proc. Natl. Acad. Sci. U.S.A.* **2005**, *102*, 16650–16655.
- Neuweiler, H.; Banachewicz, W.; Fersht, A. R. *Proc. Natl. Acad. Sci. U.S.A.* **2010**, *107*, 22106–22110.
- Doose, S.; Neuweiler, H.; Sauer, M. *ChemPhysChem* **2009**, *10*, 1389–1398.
- Qu, P.; Yang, X. X.; Li, X.; Zhou, X. X.; Zhao, X. S. *J. Phys. Chem. B* **2010**, *114*, 8235–8243.
- Li, X.; Zhu, R. X.; Yu, A. C.; Zhao, X. S. *J. Phys. Chem. B* **2011**, *115*, 6265–6271.
- Zhu, R. X.; Li, X.; Zhao, X. S.; Yu, A. C. *J. Phys. Chem. B* **2011**, *115*, 5001–5007.
- Chen, H.; Ahsan, S. S.; Santiago-Berrios, M. E. B.; Abruna, H. D.; Webb, W. W. *J. Am. Chem. Soc.* **2010**, *132*, 7244–7245.
- Jean, J. M.; Hall, K. B. *Proc. Natl. Acad. Sci. U.S.A.* **2001**, *98*, 37–41.
- Fiebig, T.; Wan, C. Z.; Zewail, A. H. *ChemPhysChem* **2002**, *3*, 781–788.
- Wan, C. Z.; Fiebig, T.; Kelley, S. O.; Treadway, C. R.; Barton, J. K.; Zewail, A. H. *Proc. Natl. Acad. Sci. U.S.A.* **1999**, *96*, 6014–6019.
- McEwen, D. P.; Gee, K. R.; Kang, H. C.; Neubig, R. R. *Anal. Biochem.* **2001**, *291*, 109–117.
- Seidel, C. A. M.; Schulz, A.; Sauer, M. H. M. *J. Phys. Chem.* **1996**, *100*, 5541–5553.
- Nazarenko, I.; Lowe, B.; Darfler, M.; Ikonomi, P.; Schuster, D.; Rashtchian, A. *Nucleic Acids Res.* **2002**, *30*, e37.
- Gotz, M.; Hess, S.; Beste, G.; Skerra, A.; Michel-Beyerle, M. E. *Biochemistry* **2002**, *41*, 4156–4164.
- Miura, T.; Urano, Y.; Tanaka, K.; Nagano, T.; Ohkubo, K.; Fukuzumi, S. *J. Am. Chem. Soc.* **2003**, *125*, 8666–8671.
- Togashi, D. M.; Szczupak, B.; Ryder, A. G.; Calvet, A.; O'Loughlin, M. J. *J. Phys. Chem. A* **2009**, *113*, 2757–2767.
- Piester, O.; Barsch, H.; Buschmann, V.; Heinlein, T.; Knemeyer, J. P.; Weston, K. D.; Sauer, M. *Nano Lett.* **2003**, *3*, 979–982.
- Neuweiler, H.; Schulz, A.; Vaiana, A. C.; Smith, J. C.; Kaul, S.; Wolfrum, J.; Sauer, M. *Angew. Chem., Int. Ed.* **2002**, *41*, 4769–4773.
- Buschmann, V.; Weston, K. D.; Sauer, M. *Bioconjugate Chem.* **2003**, *14*, 195–204.
- Doose, S.; Neuweiler, H.; Sauer, M. *ChemPhysChem* **2005**, *6*, 2277–2285.
- Qu, P.; Chen, X. D.; Zhou, X. X.; Li, X.; Zhao, X. S. *Sci. China, Ser. B: Chem.* **2009**, *52*, 1653–1659.
- Huber, R.; Fiebig, T.; Wagenknecht, H. A. *Chem. Commun.* **2003**, 1878–1879.
- Manoharan, M.; Tivel, K. L.; Zhao, M.; Nafisi, K.; Netzel, T. L. *J. Phys. Chem.* **1995**, *99*, 17461–17472.
- Marquez, C.; Pischel, U.; Nau, W. M. *Org. Lett.* **2003**, *5*, 3911–3914.
- Wanninger-Weiss, C.; Valis, L.; Wagenknecht, H. A. *Bioorg. Med. Chem.* **2008**, *16*, 100–106.
- Vaiana, A. C.; Neuweiler, H.; Schulz, A.; Wolfrum, J.; Sauer, M.; Smith, J. C. *J. Am. Chem. Soc.* **2003**, *125*, 14564–14572.
- Zhong, D. P.; Zewail, A. H. *Proc. Natl. Acad. Sci. U.S.A.* **2001**, *98*, 11867–11872.
- Shi, X.; Duft, D.; Parks, J. H. *J. Phys. Chem. B* **2008**, *112*, 12801–12815.
- Callis, P. R.; Liu, T. *Chem. Phys.* **2006**, *326*, 230–239.
- Mataga, N.; Chosrowjan, H.; Shibata, Y.; Tanaka, F. *J. Phys. Chem. B* **1998**, *102*, 7081–7084.
- Mataga, N.; Chosrowjan, H.; Shibata, Y.; Tanaka, F.; Nishina, Y.; Shiga, K. *J. Phys. Chem. B* **2000**, *104*, 10667–10677.
- Mataga, N.; Chosrowjan, H.; Taniguchi, S.; Tanaka, F.; Kido, N.; Kitamura, M. *J. Phys. Chem. B* **2002**, *106*, 8917–8920.
- Chosrowjan, H.; Taniguchi, S.; Mataga, N.; Nakanishi, T.; Haruyama, Y.; Sato, S.; Kitamura, M.; Tanaka, F. *J. Phys. Chem. B* **2010**, *114*, 6175–6182.
- Chosrowjan, H.; Taniguchi, S.; Mataga, N.; Tanaka, F.; Todoroki, D.; Kitamura, M. *J. Phys. Chem. B* **2007**, *111*, 8695–8697.
- Tanaka, F.; Chosrowjan, H.; Taniguchi, S.; Mataga, N.; Sato, K.; Nishina, Y.; Shiga, K. *J. Phys. Chem. B* **2007**, *111*, 5694–5699.
- Kim, C. H.; Park, J.; Seo, J.; Park, S. Y.; Joo, T. *J. Phys. Chem. A* **2010**, *114*, 5618–5629.
- Zhang, L. Y.; Kao, Y. T.; Qiu, W. H.; Wang, L. J.; Zhong, D. P. *J. Phys. Chem. B* **2006**, *110*, 18097–18103.
- Marme, N.; Knemeyer, J. P.; Sauer, M.; Wolfrum, J. *Bioconjugate Chem.* **2003**, *14*, 1133–1139.
- Beaumont, P. C.; Johnson, D. G.; Parsons, P. J. *J. Photochem. Photobiol., A* **1997**, *107*, 175–183.
- van de Linde, S.; Krstic, I.; Prisner, T.; Doose, S.; Heilemann, M.; Sauer, M. *Photochem. Photobiol. Sci.* **2011**, *10*, 499–506.